The Astrophysical Journal, 977:195 (10pp), 2024 December 20 https://doi.org/10.3847/1538-4357/ad89bb


# The Radio Spectra of High-luminosity Compact Symmetric Objects: Implications for Studies of Compact Jetted Active Galactic Nuclei

P. V. de la Parra[1], A. C. S Readhead[2,3], T. Herbig[4], S. Kiehlmann[3], M. L. Lister[5], V. Pavlidou[3,6], R. A. Reeves[1], A. Siemiginowska[7], A. G. Sullivan[8], T. Surti[2], A. Synani[6], K. Tassis[3,6], G. B. Taylor[9], P. N. Wilkinson[10], M. F. Aller[11], R. D. Blandford[8], N. Globus[8], C. R. Lawrence[12], B. Molina[1], S. O'Neill[13], and T. J. Pearson[2]
[1] CePIA, Astronomy Department, Universidad de Concepción, Casilla 160-C, Concepción, Chile; phvergara@udec.cl
[2] Owens Valley Radio Observatory, California Institute of Technology, Pasadena, CA 91125, USA
[3] Institute of Astrophysics, Foundation for Research and Technology-Hellas, GR-70013 Heraklion, Greece
[4] TH Masters, LLC, 136 Chichester Road, New Canaan, CT 06840, USA
[5] Department of Physics and Astronomy, Purdue University, 525 Northwestern Avenue, West Lafayette, IN 47907, USA
[6] Department of Physics and Institute of Theoretical and Computational Physics, University of Crete, 70013 Heraklion, Greece
[7] Center for Astrophysics|Harvard and Smithsonian, 60 Garden Street, Cambridge, MA 02138, USA
[8] Kavli Institute for Particle Astrophysics and Cosmology, Department of Physics, Stanford University, Stanford, CA 94305, USA
[9] Department of Physics and Astronomy, University of New Mexico, Albuquerque, NM 87131, USA
[10] Jodrell Bank Centre for Astrophysics, University of Manchester, Oxford Road, Manchester M13 9PL, UK
[11] Department of Astronomy, University of Michigan, 323 West Hall, 1085 South University Avenue, Ann Arbor, MI 48109, USA
[12] Jet Propulsion Laboratory, California Institute of Technology, 4800 Oak Grove Drive, Pasadena, CA 91109, USA
[13] Department of Physics, Princeton University, Jadwin Hall, Princeton, NJ 08540, USA
*Received 2024 August 23; revised 2024 October 16; accepted 2024 October 20; published 2024 December 12*

## Abstract

This paper addresses, for the first time, a key aspect of the phenomenology of compact symmetric objects (CSOs): the characteristics of their radio spectra. We present a radio-spectrum description of a complete sample of high-luminosity CSOs (CSO-2s), which shows that they exhibit the complete range of spectral types, including flat-spectrum sources ($\alpha \geqslant -0.5$), steep-spectrum sources ($\alpha < -0.5$), and peaked-spectrum sources. We show that there is no clear correlation between spectral type and size, but there is a correlation between the high-frequency spectral index and both object type and size. We also show that, to avoid biasing the data and to understand the various classes of active galactic nuclei (AGN) involved, the complete range of spectral types should be included in studying the general phenomenology of compact jetted AGN, and that complete samples must be used, selected over a wide range of frequencies. We discuss examples that demonstrate these points. We find that the high-frequency spectral indices of CSO-2s span $-1.3 < \alpha_{\rm hi} < -0.3$ and hence that radio spectral signatures cannot be used to discriminate definitively between CSO-2s, binary galactic nuclei, and millilensed objects, unless they have $\alpha_{\rm hi} > -0.3$.

*Unified Astronomy Thesaurus concepts:* High energy astrophysics (739)

## 1. Introduction

Although compact jetted active galactic nuclei (jetted AGN) have been intensively studied for five decades, so that much of their phenomenology is by now well known—see the comprehensive review of C. P. O'Dea & D. J. Saikia (2021)—there are still key aspects of their phenomenology that remain to be investigated (S. Kiehlmann et al. 2024a, 2024b; A. C. S. Readhead et al. 2024).

Most studies of compact radio sources focus on the typical "core jet" objects that comprise ∼90% of the compact objects in complete samples of radio sources at centimeter wavelengths (A. C. S. Readhead et al. 1978; A. C. S. Readhead 1980; T. J. Pearson & A. C. S. Readhead 1988; A. G. Polatidis et al. 1995; K. I. Kellermann et al. 1998; M. L. Lister et al. 2019). Among the classes of compact radio sources that are not "core jets," there is one that is of great interest both astrophysically and cosmologically that we focus on in this paper. These are the compact symmetric objects (CSOs; P. N. Wilkinson et al. 1994; A. C. S. Readhead et al. 1996).

S. E. Tremblay et al. (2016) showed that there are two fundamentally different classes of CSOs: an "edge-dimmed" low-luminosity class, which S. Kiehlmann et al. (2024a) designated as CSO-1s, and an "edge-brightened" high-luminosity class, which S. Kiehlmann et al. (2024a) designated as CSO-2s. In this paper, we discuss only the high-luminosity CSOs, i.e., the CSO-2s.

This paper has two basic aims: (i) to reveal the basic phenomenology of the radio spectra of CSO-2s by studying a carefully selected complete sample[14] of CSO-2s for this purpose and (ii) to demonstrate that only through the study of a number of such complete samples, selected over a wide range of frequencies, can biases be avoided, as is necessary for the underlying phenomenology to be revealed, thereby providing a firm foundation for the study of these objects.

The most obvious explanation of CSO-2s is that they represent the first stage in the evolution of double radio sources toward the larger Fanaroff–Riley type II radio sources (FR IIs; B. L. Fanaroff & J. M. Riley 1974), to which, being edge-brightened, they are morphologically very similar. However, as



[14] A "complete sample" is defined to be a sample that includes all objects down to a given flux density limit, at a specific observing frequency, and over a given area of sky (G. G. Pooley & M. Ryle 1968; M. Schmidt 1968; M. S. Longair & P. A. G. Scheuer 1970).

first pointed out by A. C. S. Readhead et al. (1994), if they are expanding at constant speed, then the numbers indicate that strong luminosity evolution is required such that, as they evolve from CSO-2s to FR IIs, their radio luminosity decreases by a factor of ∼30 while their optical narrow-line luminosity increases by about the same factor. This seems a very unlikely scenario, so we reject this evolutionary scenario for CSO-2s.

It has recently been shown that most CSO-2s are almost certainly distinct from other jetted AGN (S. Kiehlmann et al. 2024b), evolve through their whole life cycle in $\lesssim$5000 yr, and might result from tidal disruption of stars (A. C. S. Readhead et al. 2024; A. G. Sullivan et al. 2024).

In this paper, we address a basic aspect of the phenomenology of CSO-2s: their radio spectra. To do this, we examine CSO-2s in three complete samples of extragalactic radio sources. We show that about two-thirds of the objects in these samples are peaked-spectrum sources (C. P. O'Dea & D. J. Saikia 2021), while about one-third of them are compact steep-spectrum sources (J. A. Peacock & J. V. Wall 1982). We also show that ∼22% of the sources have $\alpha_{\rm hi} > -0.5$,[15] where $\alpha_{\rm hi}$ is the high-frequency spectral index as measured well above any peak or change in slope; furthermore, we find that there are roughly equal numbers of flat-spectrum ($\alpha_{5-8\ \rm GHz} \geqslant -0.5$) and steep-spectrum ($\alpha_{5-8\ \rm GHz} < -0.5$) sources in the samples we discuss.

In view of the significant fractions of both flat- and steep-spectrum sources, samples consisting of only one of these spectral types cannot be used for determining general properties of compact jetted AGN, and similarly, samples that consist of only the peaked-spectrum sources are incomplete for the purposes of determining the general phenomenology of these objects. Some previous searches for CSOs and sample studies of jetted AGN have been constructed using an initial filter of flat-spectrum objects or peaked-spectrum objects only. This has led to incompleteness; for example, some bright-core CSOs, like TXS 0128+554, were missed due to their having a flattish spectrum, while others have been missed because the spectral peak lies outside the typical radio survey window of ∼1–8 GHz.

Since the CSO classification is based solely on radio morphology, with no spectral filters applied, it provides an unbiased approach to the phenomenology of compact jetted AGN, provided that it is applied to complete samples as defined in this paper and also is applied to complete samples selected over a wide range of frequencies. We give examples of samples based on radio morphology with a spectral filter applied and/or complete samples selected over a narrow frequency range, and we point out the hazards of these approaches in each case.

The redshifts of the sources in this study range from $z = 0.05505$ to $z = 1.975$. So the 20 GHz emission luminosities of the sources discussed here range from $10^{24}$ to $10^{28}$ WHz$^{-1}$. Ultimately, one would like to have a large enough and deep enough sample of CSO-2s to be able to compare their properties in different luminosity ranges, and we are engaged on a program to do this. We are also well aware of the fact that the spectral peaks we observe translate to much higher frequencies for the high-redshift sources, and for this reason, we have undertaken studies of complete samples selected over a wide range of frequencies (from 178 MHz to 5 GHz). This program is in its infancy, and the execution of this program will take many years; for the present, we are severely restricted in this regard. For that reason, we do not attempt in this paper to address any of the redshift-dependent and/or luminosity-dependent questions that arise but only discuss those questions that can be addressed within the confines of the limited samples available at this time.

We draw attention here to the CSO B0402+379, which is unusual because it is a binary nucleus (BN; H. L. Maness et al. 2004). The separation of the binary is 7 pc, and the orbital speed is very small (∼0.001$c$; H. L. Maness et al. 2004). It does not affect the discussion in this paper, because the CSO structure is very clearly related to only one of the nuclei. Consequently, we do not differentiate between this object and the others in our sample.

For consistency with our other papers, we assume the following cosmological parameters: $H_0 = 71$ km s$^{-1}$ Mpc$^{-1}$, $\Omega_m = 0.27$, and $\Omega_\Lambda = 0.73$ (E. Komatsu et al. 2009). None of the conclusions would be changed were we to adopt the best model of the Planck Collaboration (Planck Collaboration et al. 2020).

## 2. The Three Complete Samples

In a recent study of CSOs, S. Kiehlmann et al. (2024a, 2024b) identified 18 bona fide CSOs (all CSO-2s), of which 17 have spectroscopic redshifts, in the following three complete radio samples.

(i) The Pearson–Readhead (PR; T. J. Pearson & A. C. S. Readhead 1981, 1988) sample of all 65 radio sources at declinations above $\delta = 35°$, with Galactic latitude $|b| > 10°$ and flux densities greater than 1.3 Jy at 5 GHz in the MPIfR/NRAO S4 and S5 surveys (I. I. K. Pauliny-Toth et al. 1978; H. Kuehr et al. 1981).

(ii) The first Caltech–Jodrell Bank (CJ1) sample (A. G. Polatidis et al. 1995; W. Xu et al. 1995), which extended the PR sample down to 0.7 Jy at 5 GHz and added another 135 sources to the PR sample.

(iii) The Peacock and Wall (J. A. Peacock & J. V. Wall 1981; J. V. Wall & J. A. Peacock 1985) sample (PW) of 171 sources, which is complete down to $S_{2.7\ \rm GHz} = 1.5$ Jy over the region of sky $\delta \geqslant 10°$ and $|b| \geqslant 10°$, in B1950 coordinates.

In total, there are 282 sources in these three complete samples, one of which is the starburst galaxy M82 (3C 231) and therefore not an AGN. M82 appears in the complete sample only because its small distance and the large number of supernova remnants place its radio flux density above the PW completeness limit. Thus, the parent sample of AGN that we consider below contains 281 sources.

This combined PR+CJ1+PW AGN sample of 281 sources is unique, to the best of our knowledge, in being the only high-frequency AGN radio sample of this or comparable size for which the radio structures of all of the objects are known on both large and small scales. A complete listing of this sample and its properties, together with references to maps of each object, is given by S. Kiehlmann et al. (2024b). It is the best available complete sample that includes significant numbers of flat- and steep-spectrum sources, as well as of gigahertz-peaked-spectrum (GPS) objects, and it is therefore ideal for investigating the complex ties between morphology and radio spectral shape in teasing out the complex phenomenology of

[15] We define the spectral index, $\alpha$, by $S \propto \nu^{\alpha}$.

jetted AGN. For these samples, we are now engaged in observations to triple the number of CSO-2s in complete samples and also to add complete samples selected at 178 MHz and 966 MHz.

## 3. The Radio Spectra of the CSO-2s in the PR+CJ1+PW Samples

The spectra of the 17 CSO-2s with spectroscopic redshifts in the above three complete samples (S. Kiehlmann et al. 2024a) are shown in Figure 1, displayed in order of increasing size, and corresponding maps are shown in Figure 2.

Note that the source B1333+589 does not have a spectroscopic redshift, but it does have a tentative redshift of $z = 0.57$ estimated by C. Stanghellini et al. (2009). Since this not a spectroscopic redshift, we have not used this estimated redshift in this paper.

We have pointed out that B0402+379 is unusual because it is a BN (H. L. Maness et al. 2004). However, the CSO-2 classification is related to the western nucleus, and it has clear CSO structural characteristics associated with the aligned core. The offset core contributes only ∼10% of the flux density at 5 GHz and so does not significantly affect the total spectrum.

These figures demonstrate conclusively that there is no clear relationship between spectral shape and physical size, although the larger sources do tend to peak at lower frequencies. Of interest here are (i) the numbers of flat- and steep-spectrum sources are about equal, (ii) approximately one-third of the objects do not have peaked spectra within the observed range of frequencies, (iii) some of the most compact CSO-2s do not have peaked spectra within the observed range of frequencies, and (iv) some of the most extended CSO-2s have peaked spectra.

This clearly shows that CSOs span the whole range of spectral types, including flat-spectrum sources, steep-spectrum sources, and GPS sources. In particular, we wish to emphasize the fact that not all CSO-2s are peaked-spectrum sources within the observed range of frequencies, nor do they all have flat spectra, with spectral indices $\alpha \geqslant -0.5$ at centimeter wavelengths. In the objects that do have peaked spectra, the low-frequency cutoffs are thought to be due to synchrotron self-absorption (SSA) and/or free–free absorption (FFA). Since both SSA and FFA occur in compact objects, it might be expected that the more compact objects would peak at higher frequencies, and indeed, as can be seen in Figure 3, we find that there is a clear relationship between the overall size of these CSOs and their spectral indices between 5 and 8 GHz. It is important to note that, as pointed out by A. C. S. Readhead et al. (2021), all compact radio sources *must* have a spectral turnover at some frequency. We return to these points in Section 5.

The dissection of the B2352+495 spectrum from A. C. S. Readhead et al. (1996), shown in Figure 1, was carried out using multifrequency very long baseline interferometry (VLBI) observations, shows three SSA (or FFA) cutoffs at low frequencies and three spectral aging cutoffs at high frequencies in various components, and is included to illustrate the underlying typical complexity of these spectra. The redshifts, physical sizes, and spectral indices of the 17 sources in the PR+CJ1+PW complete sample are listed in Table 1, also in order of increasing size.

The spectral indices of Figure 3 were all measured between 5 and 8 GHz using the plots of Figure 1. It is immediately clear that there is a strong inverse correlation, such that larger (more positive) spectral indices correlate with smaller size. The solid line of Figure 3 shows a linear least-squares fit to the data. The correlation coefficient is $r = -0.76^{-0.91}_{-0.43}$, with $p$-value $4 \times 10^{-4}$, where the lower and upper limits are 95% confidence limits.

We see that between 5 and 8 GHz, nine of the 17 CSOs, i.e., ∼50% in these complete samples, have spectral indices $\alpha < -0.5$, and thus that there are roughly equal numbers of flat-spectrum and steep-spectrum CSOs in complete samples selected at 5 GHz.

A. C. S. Readhead et al. (2024) showed that CSO-2s can be sub-divided into three morphological classes.

CSO 2.0s have two distinct outer lobes, making them edge-brightened, with hot spots at their outer edges opposite the nucleus, narrow jets (if jets are visible at all), and lobes not much wider than the hot spots. These are indicated by pink squares in Figure 3.

CSO 2.2s have two distinct outer lobes but the hot spots are not dominant or are invisible, or the lobes are well resolved normal to the jet axis. The hot spot or hot spots do not need to be located at the end of the lobe opposite the core. These are indicated by brown diamonds in Figure 3.

CSO 2.1s have some of the properties of CSO 2.0s and some of the properties of CSO 2.2s. For example, they might look like CSO 2.0s on one side of the nucleus and CSO 2.2s on the other side, or they might have hot spots that are not located at the extremities of their envelopes. These are indicated by green circles in Figure 3.

We see in Figure 3 that in these complete samples, CSO-2.0s in general have flatter spectra and are smaller than CSO-2.2s, and that CSO-2.1s almost span the range of CSO-2.0s and CSO-2.2s in both spectral index and size.

The spectrum of the supermassive black hole binary (SMBHB) B0402+379 (H. L. Maness et al. 2004; C. Rodriguez et al. 2006; K. Bansal et al. 2017) is shown in Figure 4. This is one of only three SMBHB candidates for which there is compelling evidence (H. L. Maness et al. 2004), the other two being B0851+202, also known as OJ 287 (A. Sillanpaa et al. 1988; M. J. Valtonen et al. 2016; L. Dey et al. 2021), and PKS 2131–021 (S. O'Neill et al. 2022; S. Kiehlmann et al. 2024c).

It is interesting to note that the spectral index of B0402+379 steepens significantly at around 2.7 GHz, from $\alpha \sim -0.35$ below 2.7 GHz to $\alpha \sim -0.65$ above 2.7 GHz. The redshift of B0402+379 is 0.05505 (R. Morganti et al. 2009), so clearly, for an object at a redshift greater than 0.05505, the spectral index above 2.7 GHz would be steep enough to exclude it from any sample with a lower cutoff on the spectral index of $\alpha = -0.5$.

This is a critical finding because it illustrates, in one object, the danger of applying spectral shape criteria in selecting samples for the elucidation of the phenomenology of compact radio sources. Among the issues discussed at the beginning of this section, we now see that spectral filters constructed using a spectral index can easily introduce redshift biases into the sample. It also makes it clear that a steep high-frequency spectrum is no guarantee against an object being an SMBHB or a millilensed galactic nucleus, because a flat-spectrum core may be dominated by the spectra of the lobes, as in this case. In order to rule out these possibilities, one needs high dynamic range maps at multiple frequencies and/or monitoring of both

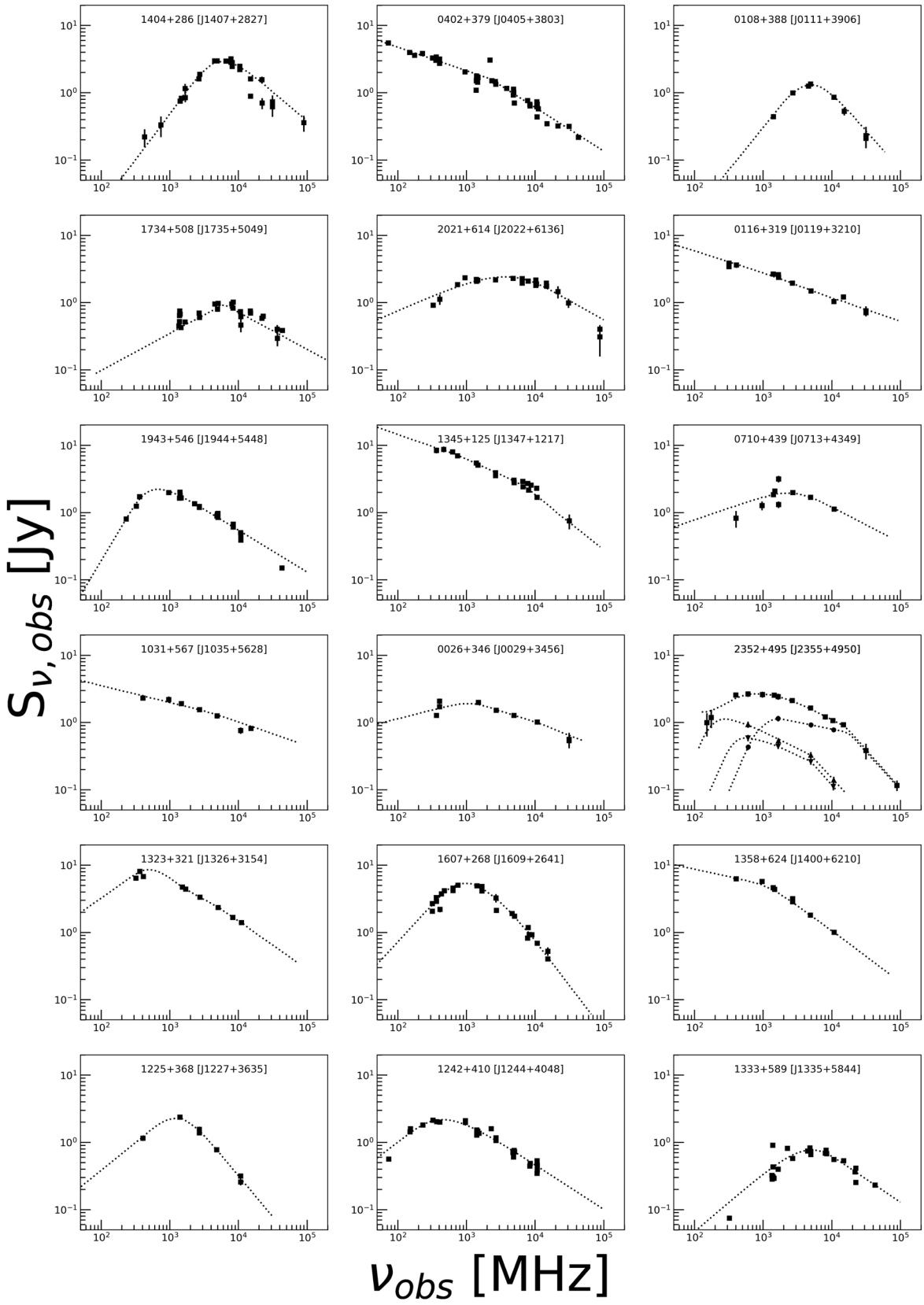


**Figure 1.** Radio spectra of the 17 CSO-2s with spectroscopic redshifts in the PR, CJ1, and PW complete samples arranged in order of increasing largest physical size from left to right in successive rows. The dotted lines show spline fits to the data. The CSO-2 B1333+589 is plotted last, since it does not have a spectroscopic redshift, so we do not know its size. These spectra are taken from T. Herbig & A. C. S. Readhead (1992), A. C. S. Readhead et al. (1996), and the CATS database (O. V. Verkhodanov et al. 2005).

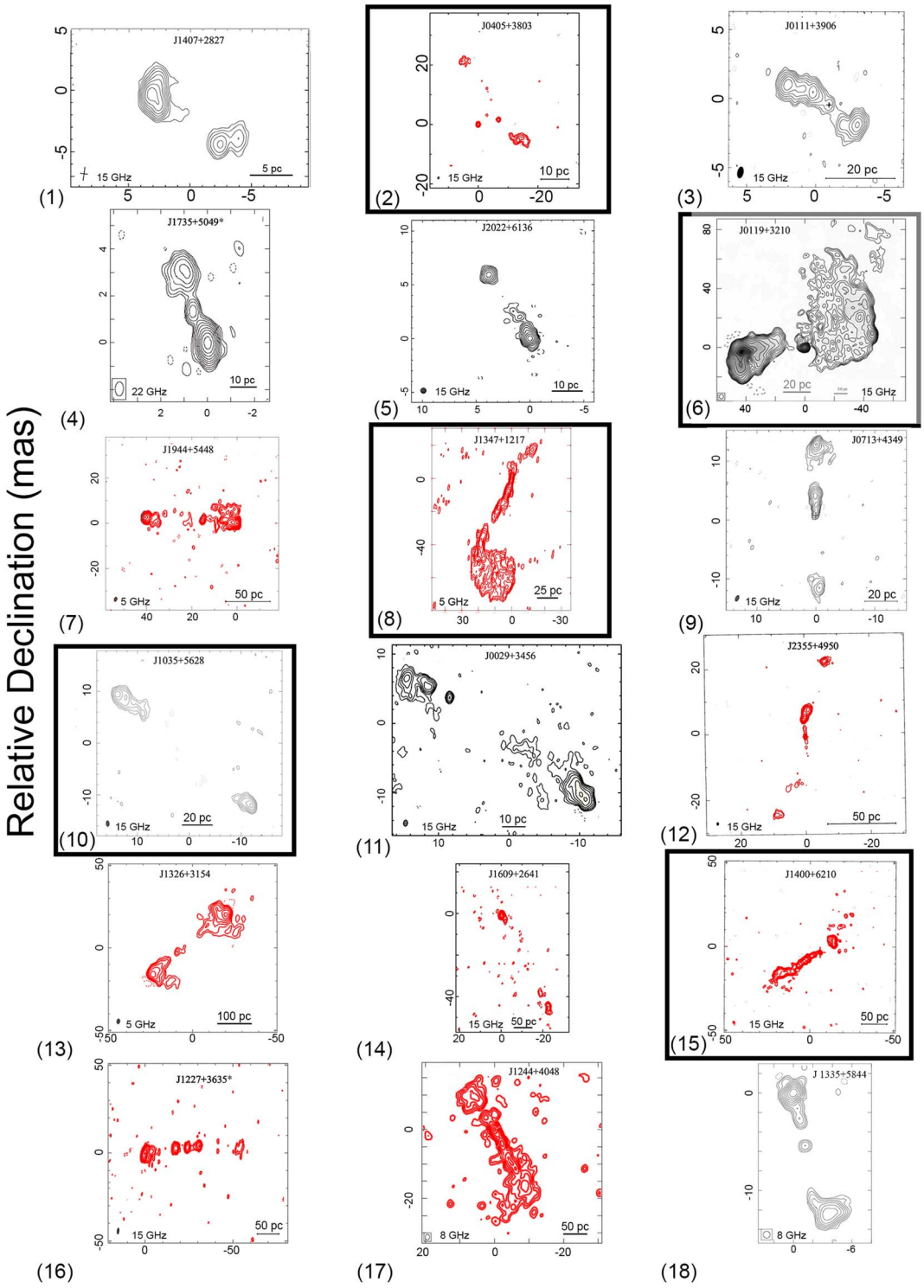


**Figure 2.** Hazards of using spectral filters in selecting samples of jetted AGN for statistically rigorous studies. Maps of the 18 CSO-2s in the PR, CJ1, and PW complete samples arranged in order of increasing size, as in Figure 1, and with B1333+589, which has no spectroscopic redshift, plotted last. The objects with red contours have steep spectra, so they would be excluded in flat-spectrum samples (see text). VLBI observations of the steep-spectrum counterpart of VIPS, corresponding to the red sources, are needed for a definitive proof/disproof the sharp cutoff in CSO-2 sizes at ∼500 pc (see text). The objects in large black boxes do not have peaked spectra in the observed range, so they would be excluded in peaked-spectrum samples (see text). The map references are as follows: (1) M. L. Lister et al. (2018), (2) H. L. Maness et al. (2004), (3) G. B. Taylor et al. (1996), (4) M. Orienti & D. Dallacasa (2014), (5) W. Tschager et al. (1999), (6) M. Giroletti et al. (2003), (7) A. G. Polatidis et al. (1995), (8) C. Stanghellini et al. (1997), (9) G. B. Taylor et al. (2000), (10) G. B. Taylor et al. (2000), (11) J. M. Marr et al. (2014), (12) G. B. Taylor et al. (1996), (13) S. E. Tremblay et al. (2016), (14) M. L. Lister et al. (2018), (15) G. B. Taylor et al. (1996), (16) W. Xu et al. (1995), (17) M. Orienti et al. (2004), (18) C. Stanghellini et al. (2009).

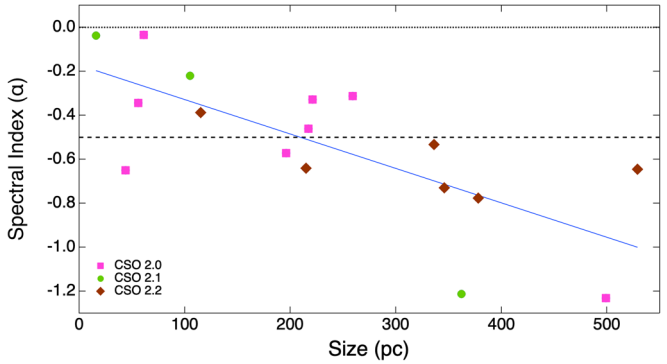


**Figure 3.** The 5–8 GHz spectral indices of the PR, CJ1, and PW CSOs plotted against their size. The pink squares are the CSO-2.0s, the green circles are the CSO-2.1s, and the brown diamonds are the CSO-2.2s. The dotted line indicates spectral index $\alpha = 0$, and the dashed line indicates $\alpha = -0.5$. The solid line is the linear least-squares fit to the data.

components of the SMBHB to determine whether or not they show the same flux density variations. In the case of B0402 +379, differing variability over 14 yr between the two compact components was required (H. L. Maness et al. 2004) to rule out millilensing.

## 4. CSO-2 X-Ray Emission

X-ray observations provide insight into the nature and environment of compact radio sources. The X-ray spectra provide a measurement of the total absorption toward the X-ray-emitting region (e.g., A. Siemiginowska 2009; L. Ostorero et al. 2017). M. Sobolewska et al. (2019) show that the most compact CSOs (<60 pc; i.e., those of approximately the size of B0108+388) have high intrinsic absorption and may reside in dense environments. Sixteen of the sources in Table 1 have X-ray data (those without are B1734+508 and B1225+368). In comparing the radio spectral index with the H I absorption column for the objects in our sample, we find no clear trend.

X-rays together with broadband modeling of the spectral energy distribution (SED) can provide constraints on emission models and discussions of the source nature. Recently, D. Ł. Król et al. (2024) investigated a model with X-ray emission originating from the compact radio lobes expanding within the dusty molecular medium. Here, the compact radio structures would be fully embedded in a dense nuclear medium. They argue that the observed X-ray radiation in this case is due to the inverse-Compton emission of the compact radio lobes with the X-ray spectral features being due to reflection of the primary continuum off the surrounding dust. They also discuss a correlation between the spectral index of the electron distribution in the lobes and the X-ray absorption column. We note that the two sources in their studies, B1404+286 and B2021+614, both have a relatively flat spectral index in Table 1 and show spectral steepening at the higher frequencies covered by their submillimeter observations. The submillimeter data were critical for constraining the electron distribution and other parameters in this model. A complete sample of compact radio sources with good SED coverage could provide a test of the origin of the broadband radiation. Note that the lobe radiation becomes less dominant in larger sources that have evolved beyond the central dusty medium.

## 5. Pitfalls of Spectrally Incomplete Radio Samples

In this section, we discuss some of the issues that can arise when one sets out to investigate the fundamental phenomenology of compact jetted AGN using spectrally incomplete samples.

### 5.1. Complete, Sufficient, and Insufficient Samples

The suitability of samples of astronomical objects for statistical tests varies in accordance with the tests applied. In studies of the general characteristics of a given class of objects, such as quasars, for example, care must be taken not to bias the study by the selection of the sample. For such studies, a "complete sample," which includes all of the objects in a given area of sky down to a given flux density limit in all of the relevant frequency bands, should be used. Complete samples, thus defined, were used, for example, in the classic papers of G. G. Pooley & M. Ryle (1968), M. Schmidt (1968), and M. S. Longair & P. A. G. Scheuer (1970).

It is important to note that G. G. Pooley & M. Ryle (1968) used a complete sample of radio sources only, selected at one frequency (408 MHz), to examine the number-flux density counts, thereby proving conclusively that bright radio sources show strong cosmological evolution, whereas M. Schmidt (1968) applied the luminosity–volume test to a complete sample of radio sources selected at 178 MHz that was also a complete optical sample to prove, using the optical magnitudes, that quasars show strong cosmological evolution. M. S. Longair & P. A. G. Scheuer (1970) then used the same sample as M. Schmidt (1968) to show that the number-flux density counts and luminosity–volume test are very closely related and are not independent tests of cosmological evolution. In all three cases, complete samples were used correctly for the particular statistical tests that were employed. Note that, while a complete sample at one frequency was sufficient to prove strong cosmological evolution of radio sources, complete samples at two frequencies were required to prove cosmological evolution of quasars.

Some studies do not require complete samples because they do not depend on detailed characterization of the objects under study. An example of such is the search for millilenses carried out by P. N. Wilkinson et al. (2001), who do not attempt to characterize the lenses other than that they are centrally condensed enough to produce multiple images through strong lensing. The characteristics of the target objects in their study are also immaterial for the purposes of their study, other than that they are compact enough to have multiple images detectable with VLBI observations.

We define a "sufficient sample" to be a sample that is both clearly defined and unbiased for the purpose of the particular study in question. The sample used by P. N. Wilkinson et al. (2001) was not complete because it included a flat-spectrum subsample, but it was sufficient for the purposes of their study because the flat-spectrum criterion did not introduce any effects that could bias the outcome.

We give below two important examples related to studies of CSOs. In the first, an insufficient flat-spectrum sample is considered and shown to have serious limitations; in the second, a limited frequency range is used to define a complete sample at only one frequency, which is again shown to be insufficient for the purposes of the study. We also point out that peaked-spectrum sources have the same hazards as, for

**Table 1**
Spectral Indices and Sizes of the CSO-2s in the PR, CJ1, and PW Samples

| B1950 | J2000 | Spectral Index ($\alpha_{2.7-5}$) | Spectral Index ($\alpha_{5-8}$) | Redshift | Size (pc) | Class | PR | CJ1 | PW |
|---|---|---|---|---|---|---|---|---|---|
| B1404+286 | J1407+2827 | 0.803 | −0.037 | 0.077 | 16 | CSO-2.1 | ⋯ | ⋯ | Y |
| B0402+379 | J0405+3803 | −0.65 | −0.65 | 0.05505 | 44 | CSO-2.0 | ⋯ | Y | ⋯ |
| B0108+388 | J0111+3906 | 0.471 | −0.344 | 0.668 | 56 | CSO-2.0 | Y | ⋯ | ⋯ |
| B1734+508 | J1735+5049 | 0.543 | −0.035 | 0.835 | 61 | CSO-2.0 | ⋯ | Y | ⋯ |
| B2021+614 | J2022+6136 | 0.012 | −0.22 | 0.227 | 105 | CSO-2.1 | Y | ⋯ | Y |
| B0116+319 | J0119+3210 | −0.38 | −0.387 | 0.0602 | 115 | CSO-2.2 | ⋯ | ⋯ | Y |
| B1943+546 | J1944+5448 | −0.571 | −0.571 | 0.263 | 196 | CSO-2.0 | ⋯ | Y | ⋯ |
| B1345+125 | J1347+1217 | −0.46 | −0.641 | 0.121 | 215 | CSO-2.2 | ⋯ | ⋯ | Y |
| B0710+439 | J0713+4349 | −0.269 | −0.46 | 0.518 | 217 | CSO-2.0 | Y | ⋯ | Y |
| B1031+567 | J1035+5628 | −0.3 | −0.328 | 0.46 | 221 | CSO-2.0 | Y | ⋯ | Y |
| B0026+346 | J0029+3456 | −0.324 | −0.313 | 0.517 | 259 | CSO-2.0 | ⋯ | ⋯ | Y |
| B2352+495 | J2355+4950 | −0.439 | −0.533 | 0.237 | 336 | CSO-2.2 | Y | ⋯ | Y |
| B1323+321 | J1326+3154 | −0.551 | −0.73 | 0.37 | 346 | CSO-2.2 | ⋯ | ⋯ | Y |
| B1607+268 | J1609+2641 | −0.973 | −1.212 | 0.473 | 362 | CSO-2.1 | ⋯ | ⋯ | Y |
| B1358+624 | J1400+6210 | −0.746 | −0.777 | 0.431 | 378 | CSO-2.2 | Y | ⋯ | Y |
| B1225+368 | J1227+3635 | −1.11 | −1.232 | 1.975 | 499 | CSO-2.0 | ⋯ | Y | Y |
| B1242+410 | J1244+4048 | −0.62 | −0.645 | 0.8135 | 529 | CSO-2.2 | ⋯ | Y | ⋯ |
| B1333+589 | J1335+5844 | 0.304 | −0.206 | ⋯ | ⋯ | CSO-2.0 | ⋯ | Y | ⋯ |

**Note.** The spectral indices were derived from fitting the data points observed at 2.7, 5, and 8 GHz shown in Figure 1, ensuring that the slope accurately represents the spectral characteristics within this frequency range. The uncertainties in the spectral indices are ∼±0.05. The sizes and redshifts are taken from Table 3 of S. Kiehlmann et al. (2024a).

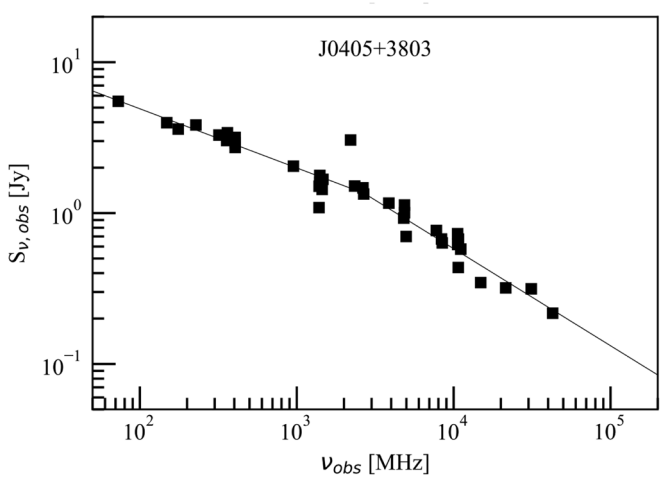


**Figure 4.** The spectrum of the SMBHB B0402+379. Below 2.7 GHz, the spectral index is $\alpha = -0.35$, whereas above 2.7 GHz, the spectral index is $\alpha = -0.65$.

example, flat-spectrum samples. We show that the result of these spectral filters is that critical members of the populations under study are likely to be excluded, thereby biasing the conclusions.

### 5.2. Flat-spectrum ($\alpha \geqslant -0.5$) and Peaked-spectrum Samples

Early VLBI surveys of compact radio sources focused on complete samples (T. J. Pearson & A. C. S. Readhead 1981; A. G. Polatidis et al. 1995). Thereafter, it was correctly thought that searches for SMBHBs and gravitational millilenses would be more efficient were they to focus on flat-spectrum sources, with spectral indices $\alpha \geqslant -0.5$, because these automatically select for compact, core-dominated objects. This approach was adopted in the Caltech–Jodrell flat-spectrum survey (CJF; G. B. Taylor et al. 1994), the CLASS survey (I. W. A. Browne et al. 2003; S. T. Myers et al. 2003), and the Very Long Baseline Array (VLBA) imaging and polarimetry survey (VIPS; J. F. Helmboldt et al. 2007).

It is clear from Figure 3 that about half of the CSOs will be missed in any sample selected at centimeter wavelengths that excludes steep-spectrum sources with spectral indices $\alpha < -0.5$. Therefore, the CJF, CLASS, and VIPS samples have likely missed about half of the CSOs that would be found in complete samples down to their flux density limits. It is therefore clearly essential to include the steep-spectrum sources in any studies of CSOs that one wishes to use in statistical or phenomenological studies of the CSO-2 class.

We now explore one consequence for statistical studies of selecting a flat-spectrum sample in more detail. In the VIPS survey, J. F. Helmboldt et al. (2007) and S. E. Tremblay et al. (2016) defined a sample of 1127 flat-spectrum sources ($\alpha \geqslant -0.5$) from the CLASS survey (I. W. A. Browne et al. 2003; S. T. Myers et al. 2003) and observed all 1127 sources at 5 GHz on the VLBA. They subsequently did follow-up studies on CSO and SMBHB candidates at multiple frequencies and discovered 20 new CSOs. So this program was successful for the purpose of efficient discovery of CSOs, but it was less helpful for the purpose of understanding the phenomenology of CSOs. For example, there are 11 VIPS CSO-2s that are not in the PR+CJ1+PW sample, and all but one of these has a size of less than 500 pc. For the sake of argument, if we were to ignore the possible biases and add these VIPS CSO-2s to the 17 CSO-2s in the PR+CJ1+PW sample, which also has only one CSO-2 of a size >500 pc, then there would be 26 out of 28 CSO-2s in the resulting sample with a size of <500 pc. The binomial probability of this 26:2 ratio is $P = 1.4 \times 10^{-6}$, i.e., a $4.7\sigma$ result, which would amount to a compelling confirmation of the ∼500 pc size cutoff in CSO-2s found by S. Kiehlmann et al. (2024b). However, from Figure 3 and Table 1, we see that roughly half the CSO-2s in complete samples have steep high-frequency spectra, so they would have been excluded by the VIPS steep-spectrum cutoff. We also see from Figure 3 that the size of the CSO-2s increases with a steepening radio spectrum.

We have applied for observing time for the steep-spectrum counterpart of the VIPS sample. We refer to this new complete sample, composed of both the flat- and the steep-spectrum sources in the VIPS footprint with $S_{8\,\mathrm{GHz}} \geqslant 85$ mJy, as the Extended VIPS (EVIPS) sample. The EVIPS sample contains 2121 sources. It is to be expected that the EVIPS sample will contain approximately twice as many CSOs as the original VIPS sample. It is entirely possible that a significant fraction of the EVIPs steep-spectrum CSOs will have sizes greater than 500 pc. If, for example, all of the expected 11 sources have sizes greater than 500 pc, then there would be 26 sources with sizes less than 500 pc and 12 sources with sizes greater than 500 pc, and the probability rises to 0.01, i.e., only a $2.3\sigma$ result —down from the $P = 1.7 \times 10^{-4}$ ($3.6\sigma$) result of S. Kiehlmann et al. (2024b). This would, in our view, significantly dilute the evidence for a sharp cutoff in sizes.

The size of the EVIPS sample (2121 sources) may be compared to the complete sample of 281 sources discussed by S. Kiehlmann et al. (2024b). If the EVIPS steep-spectrum CSO-2s show the same size distribution as the present complete sample and the same size distribution as the VIPS flat-spectrum sources, then the level of significance will increase to a $p$-value of $\sim 2 \times 10^{-9}$ ($\sim 6\sigma$), leaving virtually no room for doubt about the size cutoff observed by S. Kiehlmann et al. (2024b) and hence of the *distinctive* nature of the majority of CSO-2s.

It is clear from the discussion in this section that samples based on peaked-spectrum sources will suffer the same fate as flat-spectrum samples or steep-spectrum samples because they will miss a significant fraction of the populations under study, thereby potentially biasing the results.

We have included the above flat-spectrum sample example for three reasons: (i) to demonstrate that the test we are proposing could disprove or prove the sharp size cutoff and hence the distinctive nature of most CSO-2s; (ii) to emphasize the point that the inclusion of a radio spectrum filter can, in principle, dramatically bias the basic phenomenology under study; and (iii) to make a compelling case for follow-up of the sharp cutoff in the CSO-2 size distribution found by S. Kiehlmann et al. (2024b), which we turn to next.

#### 5.2.1. Verification or Disproof of the CSO-2 Size Cutoff

The fact that the apparent size cutoff in CSO-2s found by S. Kiehlmann et al. (2024b) is only a factor of $\sim 2$ below the upper cutoff at 1 kpc that defines the class is no coincidence. The upper size limit of 1 kpc was set by A. C. S. Readhead et al. (1996) based on the first five CSO candidates, of which four are confirmed as CSO-2.0s: B0108+388 (56 pc), B0710+439 (217 pc), B1358+624 (378 pc), and B2352+495 (336 pc). The fifth source, B0404+768 (634 pc), was later rejected as a bona fide CSO by S. Kiehlmann et al. (2024a) due to its size, which exceeded the criteria for the CSO classification.

It appeared at that time, therefore, that there was an upper cutoff in the sizes of CSO-2s at around 500–600 pc. However, since the numbers were based on only five objects, it was decided by those authors to set the upper size limit criterion for classification as a CSO at 1 kpc in order to allow for some CSOs that might be larger than those that had been discovered up to that time. S. Kiehlmann et al. (2024b) have now found a statistically significant reduction, at $p$-value $= 1.7 \times 10^{-4}$ ($3.6\sigma$), in the numbers of CSO-2s in the 500 pc–1 kpc size range. In the three complete samples described in Section 5.1, there are 17 CSO-2s, i.e., an increase in the size of the sample by more than a factor of 3 over the five objects studied by A. C. S. Readhead et al. (1996), and these 17 CSO-2s show the same size distribution as the first four listed above. The careful statistical evaluation of the size distribution of these 17 CSOs, using both the Kolmogorov–Smirnoff test and the binomial test, returned the above numbers. It is clearly important to test whether the observed size cutoff is real or due to the small size of this sample. By more than trebling the sample size, to $\sim 61$ CSOs, it should be possible to settle this question once and for all. A VLBA proposal to do just this is pending. Verification of the size cutoff would provide compelling proof that the vast majority of CSO-2s are distinct from the other classes of jetted AGN. An upper cutoff in size implies an upper cutoff in energy, raising the fascinating possibility that most CSO-2s are formed by the capture and tidal disruption of a single star by a latent SMBH (A. C. S. Readhead et al. 1994, 2024; T. An & W. A. Baan 2012; A. G. Sullivan et al. 2024).

### 5.3. Samples Selected at Only One Frequency

Inspection of Figure 1 shows that half of the CSO-2s in this complete sample would be missed, were we to use a flux-density-limited sample of sources with $S_{100\,\mathrm{MHz}} \geqslant 0.7$ Jy (i.e., the same flux density cutoff that we have used at 5 GHz). It is, therefore, critically important to cover a wide range of frequencies in which the sample is complete above a specified flux density limit when exploring the phenomenology of compact jetted AGN. For this reason, we are now observing samples that are complete at 178 and 966 MHz to match those used by S. Kiehlmann et al. (2024a) at 2.7 and 5 GHz.

## 6. Discriminating between CSOs, BNs, and Millilensed Objects

### 6.1. Radio Spectrum Discrimination

An important aspect of compact jetted AGN studies is that of searching for BNs and millilenses in the mass range $10^6$–$3 \times 10^9\,M_\odot$ (P. N. Wilkinson et al. 2001; C. Casadio et al. 2021; F. M. Pötzl et al. 2024). CSO-2s are the most serious contaminating objects in such searches.

One potential method of discriminating CSO-2s from BNs and millilenses is the high-frequency spectral index, i.e., the spectral index at the top end of the observed spectrum, above the region affected by any peak or break in the spectrum. These high-frequency spectral slopes were estimated by eye in straightforward cases and using least-squares fits if the fit by eye was not obvious. Note that these spectral indices are not the same as the $\alpha_{5-8}$ values of Table 1. The high-frequency spectral index distribution of the 18 CSO-2s in the complete samples discussed in Section 5.1 is shown in Figure 5. We see here that the high-frequency spectral indices of CSO-2s range from $-1.3$ to $-0.3$. Therefore, when using the spectral index as a filter for eliminating CSO-2s in BN and/or millilens searches, the spectral index may possibly provide a definitive filter for objects with $\alpha > -0.3$, but it clearly does not provide a definitive filter for objects with $\alpha \leqslant -0.3$.

The number of strong millilens and/or SMBHB candidates is likely to be small (P. N. Wilkinson et al. 2001), and the astrophysical importance of finding an SMBHB or a millilens is sufficiently great that observing time at both optical and radio frequencies is likely to be awarded for any compelling candidates. Thus, the considerations discussed in this section

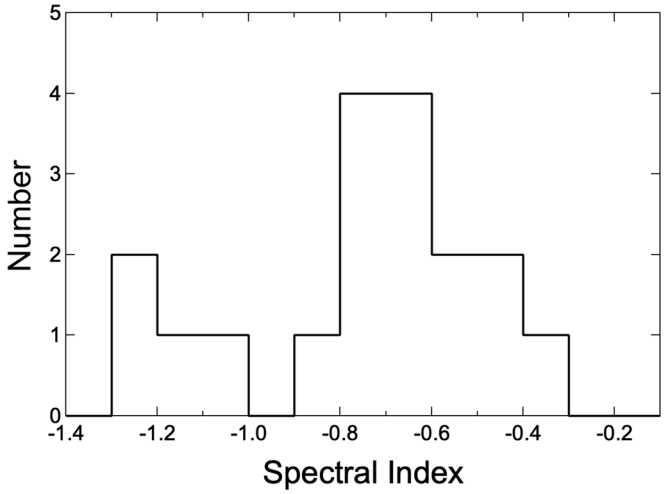


**Figure 5.** The high-frequency spectral index, $\alpha_{\rm hi}$, distribution of the PR, CJ1, and PW CSO-2s. This includes the CSO-2 1335+5844 ($\alpha_{\rm hi} = -0.70$), for which there is no spectroscopic redshift.

should serve only as a guide as to what might be happening in CSO-2s that could appear in searches for such objects and should not be used to exclude potential strong SMBHB or millilensing candidates, either of which would be an important discovery.

### 6.2. Radio Light-curve Discrimination

H. L. Maness et al. (2004) studied the variability of B0402 +379 over 14 yr with VLBI. They were able to discriminate between an SMBHB and a millilens because the two components that they were interested in were the two core components, which showed appreciably different variability over the 14 yr timescale. In the results of H. L. Maness et al. (2004), it can be seen that the two lobes show very little variability, and it would almost certainly not be possible to discriminate between these and a slowly varying millilensed system. The lobes of most CSOs vary only slowly, if at all, so this degeneracy between CSOs/SMBHBs/millilenses can be very hard to break without VLBI observations extending over at least a decade, and preferably two decades, in such cases.

## 7. Discussion

We have shown that the radio spectra of complete samples of CSO-2 objects cover the whole range of radio spectral types, including flat-spectrum, steep-spectrum, and peaked-spectrum sources. We have also shown that the CSO-2 sources that are not peaked, amounting to ∼one-third of them, span the range of sizes and are not predominantly found at the large end of the size range, as might have been expected. We have also shown that the 5–8 GHz spectral indices of CSO-2s show a strong correlation with size. We conclude that it is extremely important in studies of the phenomenology of compact jetted AGN not to introduce spectral filters of any type into the source selection, as this can bias the outcome.

It is clearly important to test whether the sharp cutoff in the CSO-2 size distribution discovered by S. Kiehlmann et al. (2024b) is real or due to the small sample, so this should be vigorously pursued. We are now engaged in observations to triple the numbers of CSO-2s in complete samples and also to add complete samples selected at 178 MHz and 966 MHz. Verification of the size cutoff would provide compelling proof that the vast majority of CSO-2s are distinct from the other classes of jetted AGN, and if proven, it could prove a watershed for AGN studies. It would put a spotlight on the population of compact radio sources in which the observed emission is not strongly beamed toward the observer, and in the case of the smallest CSO-2s, we would see significant structural evolution on a timescale of years. Such studies would enable, for the first time, direct testing of both the theory and the simulations of evolving relativistic jets in AGN, which otherwise remain virtually untestable in the critical phases of the initial launching of the jet, and the life cycle evolution of double radio sources.

## Acknowledgments

G.T. acknowledges support for this research by NASA through Fermi guest investigator grant 80NSSC22K1939. N.G. acknowledges support by the Simons Foundation (00001470). R.R., B.M., and P.V.d.l.P. acknowledge support from ANID Basal AFB-170002, Núcleo Milenio TITANs (NCN2023_002), and CATA BASAL FB210003. P.V.d.l.P. also acknowledges support by the National Agency for Research and Development (ANID)/Scholarship Program/Doctorado Nacional/2023–21232103. A.S. was supported by NASA contract to the Chandra X-ray Center NAS8-03060. In addition, the authors gratefully acknowledge the support provided by the National Science Foundation (NSF) grants AST-2407603 and AST-2407604. This paper depended on a very large amount of VLBI data, almost all of which was taken with the Very Long Baseline Array. The National Radio Astronomy Observatory is a facility of the National Science Foundation operated under cooperative agreement by Associated Universities, Inc. Parts of the work were carried out at the Jet Propulsion Laboratory, California Institute of Technology, under a contract with the National Aeronautics and Space Administration.

## ORCID iDs

P. V. de la Parra https://orcid.org/0000-0001-5957-1412
A. C. S Readhead https://orcid.org/0000-0001-9152-961X
S. Kiehlmann https://orcid.org/0000-0001-6314-9177
M. L. Lister https://orcid.org/0000-0003-1315-3412
V. Pavlidou https://orcid.org/0000-0002-0870-1368
R. A. Reeves https://orcid.org/0000-0001-5704-271X
A. Siemiginowska https://orcid.org/0000-0002-0905-7375
A. G. Sullivan https://orcid.org/0000-0002-9545-7286
A. Synani https://orcid.org/0009-0004-2614-830X
K. Tassis https://orcid.org/0000-0002-8831-2038
G. B. Taylor https://orcid.org/0000-0001-6495-7731
M. F. Aller https://orcid.org/0000-0003-2483-2103
R. D. Blandford https://orcid.org/0000-0002-1854-5506
C. R. Lawrence https://orcid.org/0000-0002-5983-6481
B. Molina https://orcid.org/0009-0000-9963-6874
S. O'Neill https://orcid.org/0000-0003-2454-6828
T. J. Pearson https://orcid.org/0000-0001-5213-6231

## References

An, T., & Baan, W. A. 2012, ApJ, 760, 77
Bansal, K., Taylor, G. B., Peck, A. B., Zavala, R. T., & Romani, R. W. 2017, ApJ, 843, 14
Browne, I. W. A., Wilkinson, P. N., Jackson, N. J. F., et al. 2003, MNRAS, 341, 13
Casadio, C., Blinov, D., Readhead, A. C. S., et al. 2021, MNRAS, 507, L6
Dey, L., Valtonen, M. J., Gopakumar, A., et al. 2021, MNRAS, 503, 4400
Fanaroff, B. L., & Riley, J. M. 1974, MNRAS, 167, 31P

Giroletti, M., Giovannini, G., Taylor, G. B., et al. 2003, A&A, 399, 889
Helmboldt, J. F., Taylor, G. B., Tremblay, S., et al. 2007, ApJ, 658, 203
Herbig, T., & Readhead, A. C. S. 1992, ApJS, 81, 83
Kellermann, K. I., Vermeulen, R. C., Zensus, J. A., & Cohen, M. H. 1998, AJ, 115, 1295
Kiehlmann, S., de la Parra, P. V., Sullivan, A., et al. 2024c, arXiv:2407.09647
Kiehlmann, S., Lister, M. L., Readhead, A. C. S., et al. 2024a, ApJ, 961, 240
Kiehlmann, S., Readhead, A. C. S., O'Neill, S., et al. 2024b, ApJ, 961, 241
Komatsu, E., Dunkley, J., Nolta, M. R., et al. 2009, ApJS, 180, 330
Król, D. Ł., Sobolewska, M., Stawarz, Ł., et al. 2024, ApJ, 966, 201
Kuehr, H., Pauliny-Toth, I. I. K., Witzel, A., & Schmidt, J. 1981, AJ, 86, 854
Lister, M. L., Aller, M. F., Aller, H. D., et al. 2018, ApJS, 234, 12
Lister, M. L., Homan, D. C., Hovatta, T., et al. 2019, ApJ, 874, 43
Longair, M. S., & Scheuer, P. A. G. 1970, MNRAS, 151, 45
Maness, H. L., Taylor, G. B., Zavala, R. T., Peck, A. B., & Pollack, L. K. 2004, ApJ, 602, 123
Marr, J. M., Perry, T. M., Read, J., Taylor, G. B., & Morris, A. O. 2014, ApJ, 780, 178
Morganti, R., Emonts, B., & Oosterloo, T. 2009, A&A, 496, L9
Myers, S. T., Jackson, N. J., Browne, I. W. A., et al. 2003, MNRAS, 341, 1
O'Dea, C. P., & Saikia, D. J. 2021, A&ARv, 29, 3
O'Neill, S., Kiehlmann, S., Readhead, A. C. S., et al. 2022, ApJL, 926, L35
Orienti, M., & Dallacasa, D. 2014, MNRAS, 438, 463
Orienti, M., Dallacasa, D., Fanti, C., et al. 2004, A&A, 426, 463
Ostorero, L., Morganti, R., Diaferio, A., et al. 2017, ApJ, 849, 34
Pauliny-Toth, I. I. K., Witzel, A., Preuss, E., et al. 1978, AJ, 83, 451
Peacock, J. A., & Wall, J. V. 1981, MNRAS, 194, 331
Peacock, J. A., & Wall, J. V. 1982, MNRAS, 198, 843
Pearson, T. J., & Readhead, A. C. S. 1981, ApJ, 248, 61
Pearson, T. J., & Readhead, A. C. S. 1988, ApJ, 328, 114
Planck Collaboration, Aghanim, N., Akrami, Y., et al. 2020, A&A, 641, A6
Polatidis, A. G., Wilkinson, P. N., Xu, W., et al. 1995, ApJS, 98, 1
Pooley, G. G., & Ryle, M. 1968, MNRAS, 139, 515
Pötzl, F. M., Casadio, C., Kalaitzidakis, G., et al. 2024, arXiv:2409.15229
Readhead, A. C. S. 1980, in IAU Symp. 92, Objects of High Redshift, ed. G. O. Abell & P. J. E. Peebles (Dordrecht: D. Reidel), 165
Readhead, A. C. S., Cohen, M. H., Pearson, T. J., & Wilkinson, P. N. 1978, Natur, 276, 768
Readhead, A. C. S., Kiehlmann, S., Lister, M. L., et al. 2021, AN, 342, 1185
Readhead, A. C. S., Ravi, V., Blandford, R. D., et al. 2024, ApJ, 961, 242
Readhead, A. C. S., Taylor, G. B., Xu, W., et al. 1996, ApJ, 460, 612
Readhead, A. C. S., Xu, W., Pearson, T. J., Wilkinson, P. N., & Polatidis, A. G. 1994, Proc. NRAO Workshop: Compact Extragalactic Radio Sources Vol. 17, ed. J. A. Zensus & K. I. Kellermann, (Green Bank, WV: NRAO), 17
Rodriguez, C., Taylor, G. B., Zavala, R. T., et al. 2006, ApJ, 646, 49
Schmidt, M. 1968, ApJ, 151, 393
Siemiginowska, A. 2009, AN, 330, 264
Sillanpaa, A., Haarala, S., Valtonen, M. J., Sundelius, B., & Byrd, G. G. 1988, ApJ, 325, 628
Sobolewska, M., Siemiginowska, A., Guainazzi, M., et al. 2019, ApJ, 871, 71
Stanghellini, C., Dallacasa, D., Venturi, T., An, T., & Hong, X. Y. 2009, AN, 330, 153
Stanghellini, C., O'Dea, C. P., Baum, S. A., et al. 1997, A&A, 325, 943
Sullivan, A. G., Blandford, R. D., Begelman, M. C., Birkinshaw, M., & Readhead, A. C. S. 2024, MNRAS, 528, 6302
Taylor, G. B., Marr, J. M., Pearson, T. J., & Readhead, A. C. S. 2000, ApJ, 541, 112
Taylor, G. B., Readhead, A. C. S., & Pearson, T. J. 1996, ApJ, 463, 95
Taylor, G. B., Vermeulen, R. C., Pearson, T. J., et al. 1994, ApJS, 95, 345
Tremblay, S. E., Taylor, G. B., Ortiz, A. A., et al. 2016, MNRAS, 459, 820
Tschager, W., Schilizzi, R. T., Snellen, I. A. G., et al. 1999, NewAR, 43, 681
Valtonen, M. J., Zola, S., Ciprini, S., et al. 2016, ApJL, 819, L37
Verkhodanov, O. V., Trushkin, S. A., Andernach, H., & Chernenkov, V. N. 2005, BSAO, 58, 118
Wall, J. V., & Peacock, J. A. 1985, MNRAS, 216, 173
Wilkinson, P. N., Henstock, D. R., Browne, I. W., et al. 2001, PhRvL, 86, 584
Wilkinson, P. N., Polatidis, A. G., Readhead, A. C. S., Xu, W., & Pearson, T. J. 1994, ApJL, 432, L87
Xu, W., Readhead, A. C. S., Pearson, T. J., Polatidis, A. G., & Wilkinson, P. N. 1995, ApJS, 99, 297